Electrochemical Characteristics and Intercalation Mechanism of Manganese Carbonate as Anode Material for Lithium-Ion Batteries

Lianyi Shao, Jie Shu[*]*, Rui Ma, Miao Shui, Lu Hou, Kaiqiang Wu, Dongjie Wang, Yuanlong Ren*

Faculty of Materials Science and Chemical Engineering, Ningbo University, Ningbo 315211, Zhejiang Province, People's Republic of China
[*]E-mail: sergio_shu@hotmail.com; shujie@nbu.edu.cn

In this paper, manganese carbonate is used as a lithium storage material for lithium-ion batteries. The electrochemical properties of manganese carbonate are studied by cyclic voltammetry and galvanostatic charge-discharge technique. The electrochemical results show that manganese carbonate has a high initial capacity of 1534.6 mAh·g^{-1}. By using ex-situ infrared method and ex-situ X-ray diffraction technique, the electrochemical reaction mechanism of manganese carbonate with lithium is a reversible conversion between Mn^{2+} and Mn^0. The electrochemical reaction between lithium and manganese carbonate can lead to the formation of manganese metal and lithium carbonate. In the reverse charge process, manganese metal and lithium carbonate can return back to lithium and manganese carbonate. Therefore, it is expected that manganese carbonate can be a promising anode material for lithium-ion batteries.

1. INTRODUCTION

Along with the rapid development of information technology and vehicle industry, energy crisis becomes more and more serious at the present day. At the same time, people pays more attention to environmental protection, As a result, how to efficient use clean energy becomes a hot research topic at the present day. Contributed to the characteristics of high capacity and superior stability, lithium-ion batteries have played a crucial role in new energy industry, electric vehicles, environmental protection and other fields. Among all the components of lithium-ion batteries, anode material is one

of the most important part attributed to its low cost and high capacity characteristics. Thus, it is necessary to explore novel promising anode materials for lithium-ion batteries.

Manganese oxide, such as MnO or MnO_2, is a kind of attractive electrode materials because of the advantages of high conductivity, high theoretical capacity (>300 mAh·g^{-1}), high energy density, low cost, low toxicity and abundant resources [1-5]. Contributed to these advantages, Mn-based active materials have been widely used in lithium primary cell. Nowadays, manganese oxide gradually becomes the active materials of the cathode in secondary lithium-ion batteries. However, it has many serious problems in practical commercial application field, such as poor cycle calendar life and low reversible capacity. For comparison, manganese carbonate is another new active material for lithium-ion batteries due to its high theoretical capacity based on a conversion topotaxial reaction. Therefore, it may be a promising anode material for rechargeable lithium-ion batteries.

In this work, we not only observe the physical properties of manganese carbonate by using Fourier transform infrared (FTIR) spectroscopy and X-ray diffraction (XRD) method, but also study the electrochemical properties of manganese carbonate through cyclic voltammetry and galvanostatic charge-discharge technique. In addition, we use the ex-situ infrared and ex-situ X-ray diffraction techniques to get a better understanding on the working mechanism of manganese carbonate as anode material for lithium-ion batteries.

2. EXPERIMENTAL SECTION

2.1 Structural and morphological characterization

Commercial $MnCO_3$ used in the experiment was purchased from Sinopharm Chemical Reagent Shanghai Co. Ltd in China. FTIR spectra were obtained by a Shimadzu FTIR-8900 spectrometer with the wavenumber range from 400 to 4000 cm^{-1}. The lithiated and delitiated samples for ex-situ FTIR study are washed by dimethyl carbonate and vacuummed for 2 h before mixing with KBr. XRD patterns were carried out using a Bruker AXS D8 Focus diffractometer with Cu Kα radiation (λ= 0.15406 nm), operating at 40 kV and 40 mA. A scan angle range between 10 and 80°, a step size of 0.1°, and a count time of 1 s were used in the experiment. The scanning electron microscopy (SEM) images were obtained with a JEOL S3400 instrument working at 10.0 kV. Thermogravimetric (TG) and differential thermal analysis (DTA) curves were obtained by a Seiko TG/DTA 6300 instrument under argon atmosphere.

2.2 Electrochemical characterization

First of all, working electrodes were prepared as follows: a moderate amount of N-methyl-pyrrolidone were added to a 8:1:1 (by mass) mixture of active material (manganese carbonate), binder (polyvinylidene fluoride) and carbon black to form a homogeneous slurry. The resultant slurry were evenly coated on the copper foil and dried at 120 ℃ under vacuum for at least 12 h and then cut into discs with a diameter of 15 mm. The simulated batteries were assembled in an Ar-filled glove box,

using manganese carbonate as cathode, lithium metal as anode, Whatman glass fiber as separator and 1 mol·dm^{-3} solution of LiPF$_6$ as electrolyte. The LiPF$_6$ solution was composed of ethylene carbonate (EC) and dimethyl carbonate (DMC) with a volume proportion of 1:1.

Galvanostatic charge-discharge cycles for simulated batteries were gained by multi-channel Land battery test system (Wuhan Jinnuo, China). All the simulated batteries were charged and discharged in 0.0-3.0 V at room temperature by using a constant current density of 50 mAh·g^{-1}. Besides, cyclic voltammograms were obtained by a CHI 1000B electrochemical workstation (Shanghai Chenhua, China).
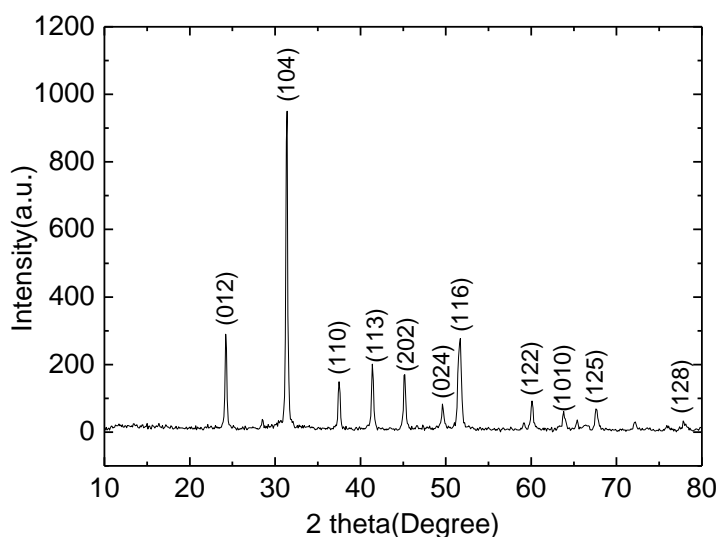
3. RESULTS AND DISCUSSION

Figure 1. XRD pattern of commercial manganese carbonate.
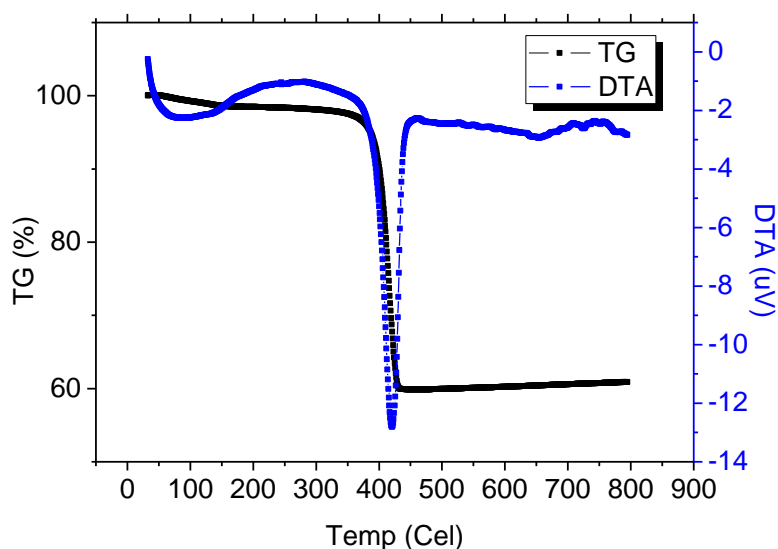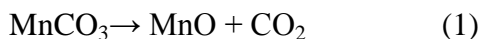

Figure 2. TG-DTA curves of manganese carbonate.

The XRD pattern of manganese carbonate is shown in Fig.1. It is a typical calcite-type Rhombohedral structure compound with the three strongest reflections at (104), (012) and (116) lines. This pattern is in good agreement with the JCPDS card No. 86-0173 and the previous reports [5,6]. The cell parameters of Rhombohedral manganese carbonate is a= 4.778 Å, c=15.642 Å, and its space group is $R\bar{3}c$(167).

The TG-DTA curves for manganese carbonate are recorded in Fig.2. As shown in this Figure, the thermal decomposition process of manganese carbonate has only one step [7,8]:

$$MnCO_3 \rightarrow MnO + CO_2 \qquad (1)$$

On the basis of the DTA curve, the thermal decomposition reaction is an endothermic reaction. The calcite-type Rhombohedral structure of manganese carbonate starts to decompose at around 370 ^{0}C. Reaction (1) finishes at about 430 ^{0}C with a total weight loss of 49.81 %.
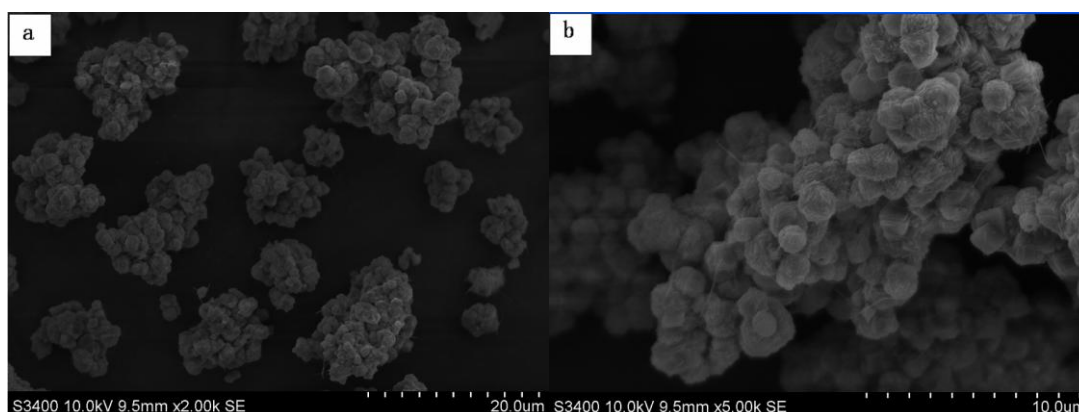

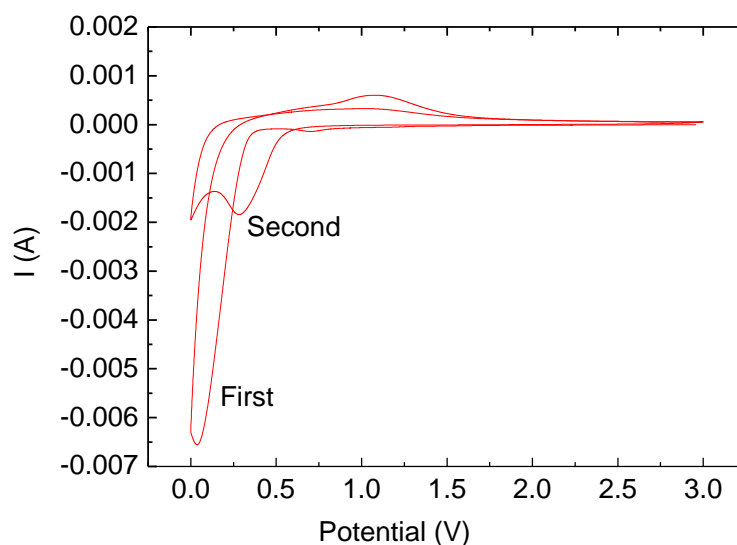**Figure 3.** SEM micrographs of manganese carbonate.

Figure 4. Cyclic voltammogram curves of manganese carbonate.

The surface morphology of manganese carbonate is shown in Fig.3. Without sample pretreatment, the surface of manganese carbonate particles is spherical shape but not smooth. It is obvious that manganese carbonate particles with an average size of about 1 μm agglomerating together to form a secondary particle. These secondary particles have an average particle size between 10 and 20 μm.

Fig.4 illustrates the initial two cyclic voltammograms of manganese carbonate at a scan rate of 1×10^{-4} V·s^{-1}. This profile is similar with the electrochemical behaviors of MnO as reported by Wang [9]. However, no cyclic voltammogram of manganese carbonate has ever been reported as anode material for lithium-ion batteries in the past ten years [5,7,8,10]. As shown in Fig.4, the first reduction scanning process appears a broad peak at 0.04 V. A sharp peak at 0.01 V and a broad peak at 0.29 V are shown in the second reduction scanning process. The decrease of reduction peak current and the shift of peak potential indicate the presence of a partial irreversible phase transition during the electrochemical reaction between manganese carbonate and lithium in the first and second cycles. Furthermore, it is also found that these two cyclic voltammograms both have a single broad anodic peak at around 1.10 V. The potential polarization between insertion and extraction process is about 1.0 V as shown in the cyclic voltammograms. It suggests that the extraction of lithium is difficult for lithiated manganese carbonate.
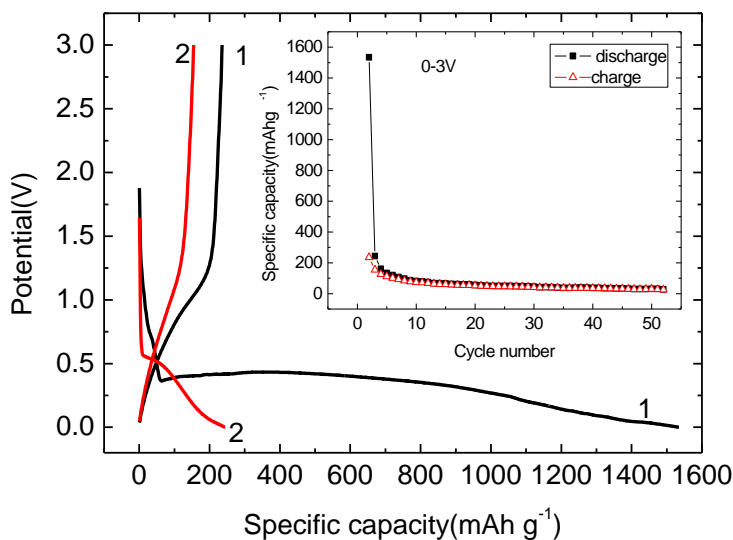

Figure 5. Charge-discharge curves of manganese carbonate at the current density of 50 mA·g^{-1}.

The electrochemical properties are further investigated by charge-discharge testing with the simulated batteries cycling at a current density of 50 mA·g^{-1} between 0.0 and 3.0 V. Fig.5 shows the charge-discharge curves of manganese carbonate as anode material for lithium-ion batteries. The first discharge voltage profile contains a sharp potential drop from 1.9 to 0.4 V and a long and flat potential plateau at about 0.38 V, occurring a reduction reaction of Mn^{2+} to Mn^{0}. This result is similar to the previous report [5]. The second discharge voltage profile deviates from the first one and reveals a slope curve. It has a higher potential plateau at around 0.5 V than the initial one. For comparison, the first

charge curve is similar with the second one. Both charge curves possess a slope potential plateau at about 1.2 V, undergoing an oxidation reaction of Mn^0 to Mn^{2+}. For each conversion electrode material, the first step can be described by using the following equation:

$$MnCO_3 + 2Li \leftrightarrow Li_2CO_3 + Mn \quad (2)$$

The relation between the cycle number and specific capacity is also studied. Viewed from the cycling results, it is found that the initial discharge specific capacity for manganese carbonate is 1534.6 $mAh \cdot g^{-1}$. In the subsequent cycles, the specific capacity decreases from 244.3 to 27.8 $mAh \cdot g^{-1}$. The charge capacity from the 2nd to 51th cycle reduces from 154.5 to 26.2 $mAh \cdot g^{-1}$. Theoretically, the initial irreversible capacity of conversion electrodes is always much larger than that of the following cycles [5]. The initial irreversible capacity for active material is 1299.2 $mAh \cdot g^{-1}$. Based on the previous reports, it is known that the initial irreversible capacity of manganese carbonate can be associated with particle pulverization, electrolyte degradation, the formation of a solid electrolyte interphase and the insertion reaction in carbon black additive [5,10]. As a result, the reversible capacity can not reach the theoretical value (466 $mA \cdot g^{-1}$) of manganese carbonate [10]. As shown in Fig.3, manganese carbonate particles aggregate together leading to a low surface area, which can not provide much more material/electrolyte interface for lithium ion diffusion. Moreover, the active particles pulverize and become electrochemically inactive materials upon repeated cycles. Therefore, only low specific capacity can be delivered after many cycles [11].
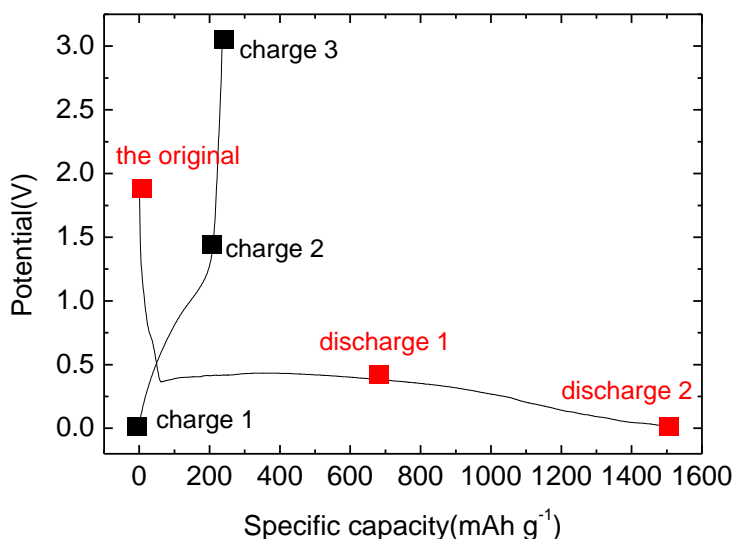

Figure 6. Six lithiated and delithiated samples obtained for ex-situ FTIR analysis in the initial charge-discharge curve.

Based on the literatures [5,7,8,10], it is known that other groups have focused on   the development of lithium storage metal carbonates materials in the past five years. However, they made few experiments on the study of the insertion/extraction mechanism of metal carbonates. In order to confirm the existence of this conversion reaction and better understand the lithium storage mechanism

in metal carbonates, we make a thoroughly investigation on the structural evolutions of manganese carbonate during charge-discharge cycles by using ex-situ FTIR and ex-situ XRD techniques.

Here, we assembled six simulated batteries in the ex-situ FTIR experiment, named the original, discharge 1, discharge 2, charge 1, charge 2 and charge 3. We prepared three lithiated samples with the names of the original, discharge 1 and discharge 2 as shown in Fig.6. In the reverse charge process, three delithiated samples are named as charge 1, charge 2 and charge 3. After charge or discharge, the forenamed slices were rinsed with DMC in an argon-filled glove box, dried under vacuum conditions at room temperature and then analyzed by FTIR technique.
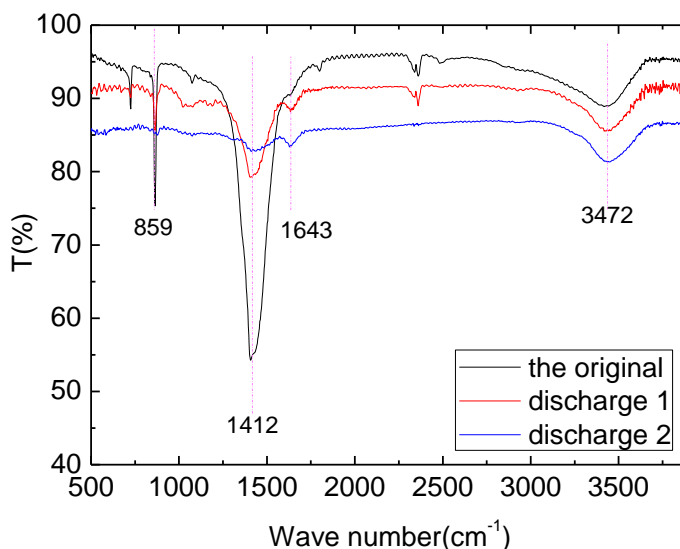

Figure 7. Ex-situ FTIR spectra of the original manganese carbonate and other two lithiated samples in the initial discharge curve.
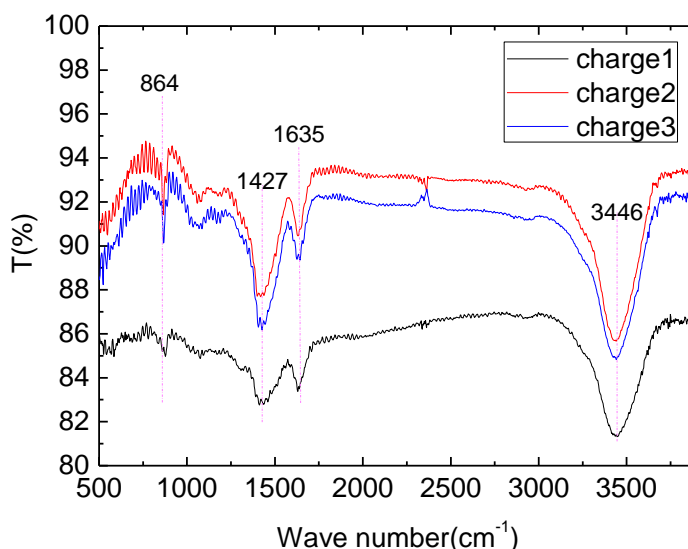

Figure 8. Ex-situ FTIR spectra of three delithiated samples in the initial charge curve.

Fig.7 and 8 show the IR spectra of the lithiated and delithiated samples for manganese carbonate. As shown in Fig.8, the weak bands at 1643 and 3472 cm^{-1} are attributed to the bending and

stretching vibrations of water molecules, respectively. The characteristic peaks at 1412 and 859 cm^{-1} are contributed to CO_3^{2-} vibrations [6,12]. With the discharge process proceeding, the intensities of characteristic peaks for CO_3^{2-} decrease gradually. It indicates that there is a transformation reaction of Mn^{2+} to Mn^0 during lithium insertion process. Viewed from Fig.8, the delithiated active materials have similar infrared feactured peaks of CO_3^{2-} in the charge process. Contrary to the discharge process, the intensities of characteristic peaks for CO_3^{2-} show a gradual strengthening in charge process due to a reverse transformation process of Mn^0 to Mn^{2+}. Based on the ex-situ FTIR results, it is obvious that the reaction mechanism of $MnCO_3$ with Li is consistent with the equation 2 mentioned above
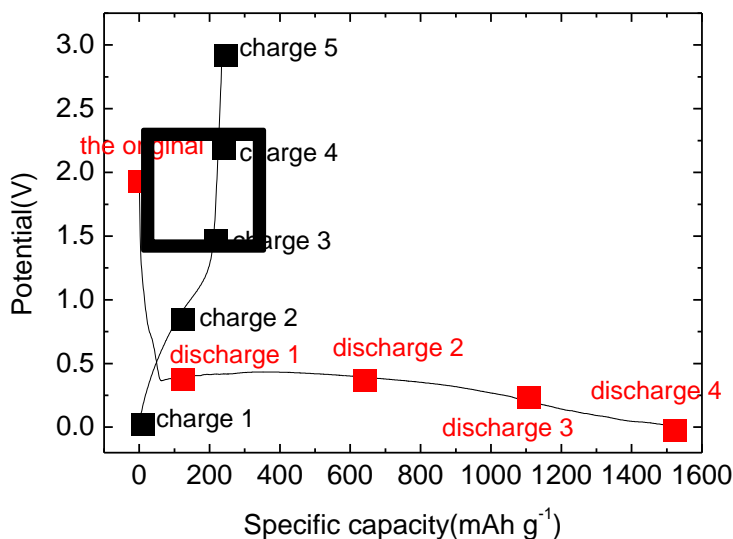

Figure 9. Ten lithiated and delithiated samples obtained for ex-situ XRD analysis in the initial charge-discharge curve.
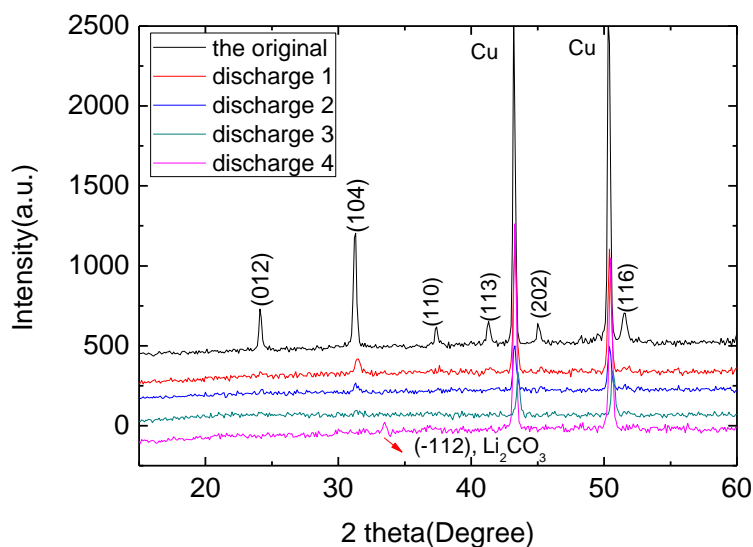

Figure 10. Ex-situ XRD patterns of the original manganese carbonate and other four lithiated samples in the initial discharge curve.

Based on the ex-situ infrared results, we make a preliminary understanding on the working mechanism of manganese carbonate in the process of charge-discharge cycles. In order to better understand the conversion reaction, we make ex-situ XRD study on the structural evolutions of active materials as anode for lithium-ion batteries. Here, we assembled 12 simulated batteries in the ex-situ XRD experiment, named the original, discharge 1, discharge 2, discharge 3, discharge 4, discharge 5, charge 1, charge 2, charge 3, charge 4, charge 5 and charge 6. We prepared five lithiated samples with the names of with the names of the original, discharge 1, discharge 2, discharge 3 and discharge 4 as shown in Fig.9. In the reverse charge process, five delithiated samples named charge 1, charge 2, charge 3, charge 4 and charge 5 are prepared as shown in Fig.9. After charge or discharge, the forenamed slices were obtained from the simulated batteries in an argon-filled glove box, dried under vacuum conditions and then studied by XRD. The ex-situ XRD patterns of five lithiated samples in discharge process are depicted in Fig.10. It is obvious that six bragg reflections attributed to (012), (104), (110), (113), (202) and (116) lines belong to the characteristic peaks of manganese carbonate. In the discharge process, the intensities of these six diffraction peaks become weaker and weaker from the original one to the discharge 4. Furthermore, a new bragg reflection can be observed in the ex-situ XRD pattern of the discharge 4 sample. According to the JCPDS card No.83-1454, we realize that this new peak belongs to the characteristic diffraction peak of lithium carbonate (Li_2CO_3), corresponding to the crystal face (-112). It indicates that the initial electrochemical transformation of Mn^{2+} to Mn^0 results in the formation of Li_2CO_3.
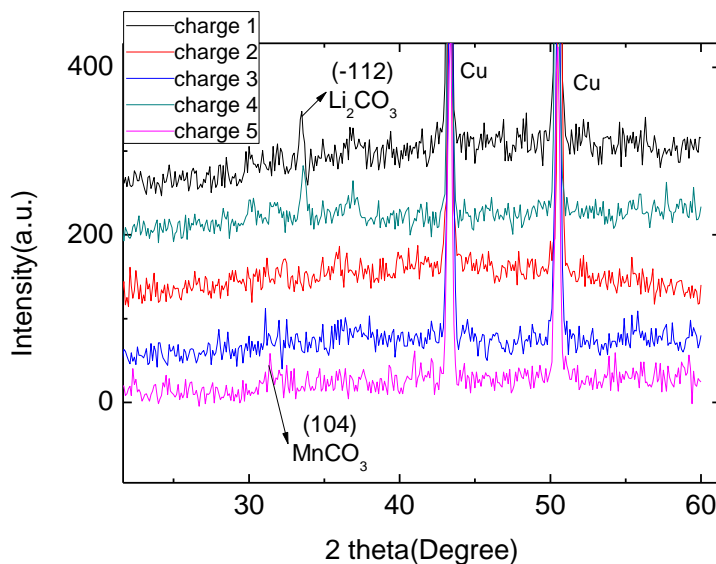

Figure 11. Ex-situ FTIR spectra of five delithiated samples in the initial charge curve.

The ex-situ XRD patterns of five delithiated samples in charge process are shown in Fig.11. As mentioned above, the discharge reaction of manganese carbonate leads to the formation of metal manganese and lithium carbonate. After a discharge process to 0.0 V, only the characteristic diffraction peak of lithium carbonate can be observed in the ex-situ XRD pattern. In the reverse charge process,

the diffraction peak at 33.4° attributed to Li_2CO_3 become weaker and weaker from the charge 1 to the charge 5. Moreover, a weak bragg reflection reappears in the XRD curve of the charge 4 and 5, which is corresponding to the characteristic (104) reflection line of manganese carbonate (JCPDS card No. 86-0173). These results suggest that the reverse transformation of Mn^0 to Mn^{2+} is feasible during the charge process. Therefore, the electrochemical reaction between manganese carbonate and lithium is reversible process shifting from manganese metal and lithium carbonate.

4. CONCLUSIONS

In our experiment, cyclic voltammogram and galvanostatic charge-discharge cycle of manganese carbonate demonstrate that metal carbonates (MCO_3, M=Mn, Fe, Co, Ni, Cu) are promising lithium storage materials as anode materials for lithium-ion batteries. The structural evolutions of manganese carbonate were observed by ex-situ XRD and ex-situ FTIR techniques during the initial charge-discharge cycle. The shift of characteristic diffraction peaks and infrared absorption peaks indicate the reversible structural conversion between Mn^{2+} and Mn^0. These results prove that the reaction of manganese carbonate with lithium can lead to the formation of manganese metal and lithium carbonate. It also shows that manganese metal and lithium carbonate can reversibly change into lithium and manganese carbonate during the charge process. In addition, the initial discharge specific capacity of manganese carbonate reaches a value of 1534.6 mAh·g^{-1}. Based on these results, it is obvious that manganese carbonate will be a promising lithium storage material for lithium-ion batteries.

References

1. R. N. Reddy, R. G. Reddy, *J. Power Sources*, 132 (2004) 315.
2. S. J. Bao, B. L. He, Y. Y. Liang, W. J. Zhou, H. L. Li, *Mater. Sci. Eng. A*, 397 (2005) 305.
3. J. Li, N. Wang, Y. Zhao, Y. Ding, L. Guan, *Electrochem. Commun.*, 13 (2011) 698.
4. M. Malisic, A. Janosevic, B. S. Paunkovica, I. Stojkovic, G. Ciric-Marjanovic, *Electrochim. Acta*, 74 (2012) 158.
5. M. J. Aragon, B. Leon, C. P. Vicente, J. L. Tirado, *J. Power Sources*, 196 (2011) 2863.
6. S. M. Pourmortazavi, M. Rahimi-Nasrabadi, A. A. Davoudi-Dehaghani, A. Javidan, M. M. Zahedi, S. Hajimirsadeghi, *Mater. Res. Bull.*, 47 (2012) 1045.
7. S. Mirhashemihaghighi, B. Leon, C. P. Vicente, J. L. Tirado, R. Stoyanova, M. Yoncheva, E. Zhecheva, R. S. Puche, E. M. Arroyo, J. R. Paz, *Inorg. Chem.*, 51 (2012) 5554.
8. M. J. Aragon, B. Leon, C. P. Vicente, J. L. Tirado, *J. Power Sources*, 189 (2009) 823.
9. B. Sun, Z. X. Chen, H. Kim, H. Ahn, G. X. Wang, *J. Power Sources*, 196 (2011) 3346.
10. M. J. Aragon, C. P. Vicente, J. L. Tirado, *Electrochem. Commun.*, 9 (2007) 1744.

11. C. H. Lu, S. W. Lin, *J. Power Sources*, 97-98 (2001) 458.
12. L. X. Yang, Y. Liang, H. Chen, Y. F. Meng, W. Jiang, *Mater. Res. Bull.*, 44 (2009) 1753.